# Analysis of the Cyclic Short-Term Variation of Indoor Power-line Channels

*Francisco Javier Cañete, José Antonio Cortés,*
*Luis Díez and José Tomás Entrambasaguas* *

**Abstract.** The purpose of this paper is to analyze the properties of indoor power-line communications (PLC) channels when they are used for broadband transmission. It will be shown that these channels exhibit a short-term variation, due to the fact that high-frequency parameters of electrical devices depend on the instantaneous amplitude of mains voltage. This phenomenon leads to a channel model proposal based on a linear periodically time-varying system and cyclostationary random noise. A measurement system, designed to capture these time variations in real power networks, and some of the most significant results obtained with it, are presented. In addition, a statistical analysis of the measurements performed in several indoor power-line scenarios is included, so that the relevance of time variations in actual channels can be evaluated.

**Keywords:** power-line communication, broadband communication, time-varying channels, home appliances measurement, LPTV systems, cyclostationary noise, frequency response.

## 1. INTRODUCTION

Nowadays, the study of indoor power lines as broadband communication channels is generating remarkable interest. This is mainly caused by the economical advantage of using them as part of the new last-mile technology over low-voltage distribution lines and, specially, by an increasing demand for in-home networking capabilities. Traditional measurements and models for this channel assume an LTI (Linear Time-Invariant) nature in which changes in the response occur only as a result of the connection or disconnection of electrical appliances to the grid, which represent long-term variations [1,2,3,4]. However, due to the periodic time-variant behavior of some devices, synchronous to the mains frequency, the channel exhibits a periodic time-varying response and cyclostationary noise components. The main goal of this paper is the characterization of the high-frequency properties of indoor power lines, putting emphasis on their short-time variation. Thus,

* The authors are with the department of *Ingeniería de Comunicaciones* - University of Málaga (SPAIN).

this work tries to complement previous ones that analyze channel performance obviating this aspect [2,3,5,6,7].

The paper is organized as follows. First of all, the low-voltage distribution network structure and its main features are concisely outlined. In section three, a behavioral model for electrical devices connected to the power grid is proposed, with linear time-varying loads and cyclostationary noise generators. Measurement results from electrical appliances that show this variation are also included. In section four, channel slow-time variation is discussed and a measurement system designed according to it, with signal processing algorithms able to extract cyclic properties, is described. Some representative measurement results of actual channels are also presented. In section five, an analogous study is provided for the received noise. Afterwards, a statistical analysis that assesses the incidence of channel time variations in real scenarios is presented in section six. Finally, some conclusions about indoor PLC channels time-varying behavior and its impact on real transmission systems are given.

## 2. INDOOR POWER NETWORKS STRUCTURE

The indoor part of the low-voltage distribution network may be seen as a structure composed of the wiring and the devices connected to it. The wires are generally deployed by means of several branch circuits that extend from the service panel to the different outlets (connection terminals), where electrical devices can be plugged. The wiring layout can be described by the relative position and length of the different line sections. Channel characteristics can be estimated under the assumption that indoor power lines are a series of interconnected transmission lines, terminated in diverse loads that model the connected devices.

Every device connected to the power network represents a terminal load that can be modeled by means of some kind of impedance function. Besides that passive feature, they also behave as generators that introduce broadband noise in the network. Actually, these can be considered the most important sources of the noise that reaches any point of the grid. Once the devices have

been modeled as loads associated to a certain outlet, the transmission and reception points completely determine the channel response. Even more, if devices behavior is known, it is possible to generate feasible PLC channels from actual devices measurements and a good characterization of the wiring [3].

It is appropriate to consider an additional term of noise at the receiver, apart from the one produced by the network devices, due to disturbances originated outside (coupled to the wires from radio stations or wireless systems emitting in the band of interest, or conducted from the service panel and due to devices in other power networks). This noise term is composed of stationary or cyclostationary components and other impulsive ones (clearly non-stationary and probably associated to transitions when connecting or disconnecting devices). The impulsive components are out of the scope of this work because they have been already studied in depth [9].

In addition, devices properties in the high-frequency range change when they are turned on/off, which cause long-term channel variations since they occur within a time scale of minutes or hours [3]. Actually, such channel dynamics can be modeled as if a new power-line network structure appears every time some appliance changes its working state. In this paper, it is assumed that there are no changes in the devices working state, so the power-line network structure is "static". We are interested only in short-term channel variations [10].

## 3. DEVICES CHARACTERIZATION

There exists a large diversity of devices that can be connected to indoor power networks. If working state changes are put aside, the voltage to current relation in some devices is linear and time-invariant (LTI), and so their load can be completely characterized by an impedance, usually frequency-dependent. However, there are many other devices with a behavior that is far from being LTI. In the same way, the noise generated by some devices is stationary and can be characterized by a certain power spectral density (PSD), while others not.

In PLC transmission systems there is a high separation, both in frequency and voltage level, of the two waveform components at any device: the AC waveform, sinusoidal with 50Hz and $230V_{rms}$ (in Europe), and the communication signal (with a voltage usually below 1V and higher frequency). Performed measurements corroborate, as expected, that home appliances high-frequency properties exhibit an appreciable nonlinear behavior only determined by the AC waveform, since the communication signal level is negligible. This leads to a device small-signal model whose parameters depend on the instantaneous value of mains voltage, and hence, are periodic in time. It comprises a cyclostationary noise source, characterized by its short-term instantaneous power spectral density $S_N(t,f)$ [11], and a linear periodically time-varying (LPTV) load, characterized by its short-term impedance $Z(t,f)$.

### 3.1. Devices load impedance measurements

In order to analyze the behavior of the appliances it is essential to synchronize the measurement system with mains voltage. The basic elements employed to measure loads impedance values are a vectorial network analyzer, a coupling circuit (to protect this instrument from the mains) and a trigger circuit [12]. The latter is required to control the analyzer frequency sweep with mains voltage (conventional measurements use a self-triggered sweep mode). Impedance values of tens of common electrical appliances have been measured with this arrangement.

Obtained results allow devices to be classified into two groups according to their behavior during the mains cycle. The first set would contain those loads that present two states of impedance value and abrupt transitions between them, probably caused by silicon control rectifiers (SCR) (for instance, low-power lamps, light dimmers, electric shavers and electric blankets can be included in this group). The impedance seems to depend on the absolute level of the mains signal, resulting in a periodicity of $2/T_0$=100Hz (in Europe). Devices of the second group exhibit impedance values with smoother time variations, usually with a periodicity of $f_0=1/T_0$=50Hz (that is the case of monitors, microwave ovens, vacuum cleaners, coffee-machines, mixers...). In both

groups, a remarkable frequency selectivity of the impedance time variations is observed [12]. Fig. 1 shows the impedance of a device of the first group, it is from an electric shaver, quite similar also to the one from some low-power lamps. As seen, the magnitude of the short-term impedance $|Z(t,f)|$ clearly exhibits the aforementioned two-state behavior during a cycle: in the 1st and 3rd quarter of the cycle[1] there are high values around 20MHz, but they move towards low frequencies in the 2nd and 4th quarter. There are changes of more than 500Ω between these two states at many frequencies.

### 3.2. Devices noise measurements

Regarding the noise generated by electrical devices, there is a great variety of appliances in the home and their associated noise processes have also quite diverse characteristics. Many devices introduce a non-relevant level of noise, while other ones are very noisy. Some have a simple electrical structure and can be modeled as stationary and gaussian (but seldom white) noise sources. On the other hand, other devices have an interface to the grid that includes circuits whose behavior is strongly dependent on the instantaneous mains signal level, which causes a periodic variation of the noise source parameters. Many SCR in appliances power-supply circuits and lighting devices, or switched-mode power supplies of electronic equipment are typical examples of this phenomenon.

The instantaneous PSD, $S_N(t,f)$, of devices emitted noise can be estimated by different measurement procedures, e.g. with a spectrum analyzer or a data acquisition instrument connected to the mains terminals of the Device Under Test (DUT) by means of a coupling circuit. In any case, it is necessary to make an averaging synchronized with mains cycle. Moreover, the DUT should be plugged into the power grid through an isolation filter that behaves as a low-pass filter that mitigates the noise from the network in the band of interest.

The analysis of a considerable number of devices reveals that the periodicity of the noise

1 Note that the 0ms time-reference of the figures corresponds to the mains signal rising zero-crossing.

instantaneous PSD can be 100Hz or 50Hz (depending on whether the devices are affected just by the absolute value of the mains voltage or also by its polarity). Fig. 2 shows the measurement of a device whose instantaneous PSD is cyclic with a period of 20ms (a mixer). Two additional features of the noise from most devices are also observed: the remarkable frequency selectivity of the time variations and the high excursion of the changes along the cycle (with more than 20dB at certain frequencies).

## 4. CHANNEL RESPONSE CHARACTERIZATION

A two-port network that consists of a set of interconnected transmission lines terminated in loads with a certain impedance (i.e. loads with an LTI behavior) can be modeled as an LTI system. Two-port network parameters can be estimated if the lines structure is characterized and, after some simple calculations, the system transfer function may be obtained [3]. When line terminations are assumed to have a nonlinear behavior, consequently, the whole power network should be described by means of a nonlinear system. Nevertheless, there exists certain conditions that facilitate the channel behavior analysis, whose mathematical basis are explained in the appendix. The first one is that, due to the periodic nature of the large component at the input (mains voltage) and its very high level, the channel can be linearized and studied as an LPTV system (see section A.1). The second one is that the slow-variation allows a simplification of the channel filtering process. Therefore, if both the input signal and the channel impulse response are short with respect to the channel coherence time, the output signal Fourier transform, $Y(f)$, is given by the following locally time-invariant approximation,

$$Y(f) \approx H(t,f)\big|_{t\approx t_0} \cdot X(f) \tag{1}$$

where $t_0$ indicates the instant of mains cycle when the input signal, with Fourier transform $X(f)$, is applied. Moreover, as a long input signal can always be divided into several shorter ones, Equation (1) only requires the channel to be "underspread" (see section A.2.1). Fortunately, measurements carried out confirm that this circumstance is loosely accomplished, as will be shown later in this work.

### 4.1. Measurement methodology

This subsection describes the methodology employed to measure the frequency response of actual indoor power-line channels. Previous results presented in the literature [1,6] have been obtained by means of procedures designed to explore LTI channels, so they show no time variation. To bring this feature to light it is necessary to carry out long-time measurements using the mains cycle as a reference, otherwise the time variation remains unveiled.

The measurement setup [13] consists of a PC with a signal generation card used as transmitter and another PC with a data acquisition card used as receiver. Both are connected to distant outlets through coupling circuits, which include transformers and high-pass filters that protect the equipment from mains voltage and behave like baluns to inject/extract differential mode signals only. They also serve as a reconstruction filter after the transmitter and as an antialiasing filter before the receiver. Transmitter and receiver cards have a 50Ω impedance value. Hence, losses due to both coupling circuits (approximately 10dB in the passband) and to impedance mismatching are measured as part of channel losses. This arrangement permits recording signal lengths equivalent to hundreds of mains cycles, which are analyzed at a later time.

The study of the channel frequency response is performed by means of a sounding signal formed by a set of $N$ harmonically related sinusoids distributed between 0Hz and 25MHz. The value of $N$ is fixed to 512, leading to a spectral resolution of $\Delta f$=25MHz/$N$=48.8kHz. However, since the passband of the coupler circuits extend from 1MHz to 20MHz, only sinusoids within this range are finally launched into the power grid.

Although the transmitted sinusoids have a constant amplitude and phase, due to the time-varying filtering process of the power-line channel, they exhibit a periodic variation at the receiver. To study this periodicity, the received signal, $y(n)$, is registered during the time of $C$ mains periods. Each cycle $c$, with $0 \le c \le C-1$, is divided into $L$ regularly distributed intervals of duration $T_\ell = T_0/L = 2NT_s$ (i.e. contains $2N$ samples taking at a rate $1/T_s$). The amplitude and phase of the

sinusoids received in the $\ell$-th interval of the $c$-th cycle is estimated by computing the $2N$-point DFT (Discrete Fourier Transform) of the signal $y_{c,\ell}(n) = y(2NLc + 2N\ell + n)$, with $0 \le n \le 2N-1$,

$$Y_c(\ell,k) = \frac{1}{2N}\sum_{n=0}^{2N-1} y_{c,l}(n)\cdot e^{-j\frac{2\pi}{2N}kn} \tag{2}$$

which, provided that the slow-variation assumption in (1) applies, can also be expressed as

$$Y_c(\ell,k) = H(\ell,k)\cdot X(k) + N_c(\ell,k) \tag{3}$$

$H(\ell,k)$ is a sampled version of the frequency response $H(t,f)\big|_{t=\ell T_\ell, f=k\Delta f}$, where $\ell \in [0, L-1]$ and $k \in [0, N-1]$ are the time index and frequency index, respectively. $X(k)$ is the Fourier series coefficient of the sinusoid transmitted at frequency $f=k\Delta f$ and $N_c(\ell,k)$ is the noise received during the $\ell$-th interval of the $c$-th cycle.

An estimate of the frequency response, $\widehat{H}(\ell,k)$, has been obtained by performing a synchronized averaging of (3),

$$\widehat{H}(\ell,k) = \frac{1}{X(k)}\frac{1}{C}\sum_{c=0}^{C-1} Y_c(\ell,k) \tag{4}$$

with $C$ fixed to 234, $L$ to 976 and, hence, a $T_\ell$ of, approximately, 20.5μs.

Additional synchronization correction algorithms have been employed to compensate for the frequency mismatch between the transmitter and the receiver clocks and for the accumulated jitter of the mains, which can not be neglected when averaging over hundreds of cycles.

The methodology described up to now assumes a linear behavior of the channel for the communication signal. To corroborate this premise it must be ensured that the possible harmonics and intermodulation products generated by the channel during the $\ell$-th interval will have different phase in each processed cycle. Since this end can not be guaranteed by transmitting constant phase sinusoids, the sounding signal and receiver algorithms have been changed to create a Discrete MultiTone (DMT) system [14]. The number of carriers has been fixed to 512 and the cyclic prefix length has been varied to obtain DMT symbols lengths, $T_{\mathrm{DMT}}$, in the range from 21.48μs to 27.50μs (short enough to comply with the slow-variation

assumption). The comparison of the frequency responses estimated with both methods confirms the linear behavior of the channel for the communication signal.

Measurements have been carried out in three different scenarios: in a university building (in laboratories and offices, where there are mainly PCs), in an apartment of about 80m$^2$ and in a detached house of about 300m$^2$. The number of registered channels, chosen between different outlets at random, exceed fifty, with a similar number of them at the mentioned locations. The devices plugged in the power network outlets during the measurements were not intentionally selected; they were in their habitual location and no additional device with a special time-varying behavior was included.

### 4.2. Representative results

In this subsection, some examples of the most representative frequency responses are studied in order to illustrate channels time variations. Provided that the channel periodic behavior is caused by devices connected to the grid, it follows that the channel responses exhibit similar tendencies in their time variation to the ones of the devices impedance. Hence, there are some with sharp changes between two states of response along a cycle, and others with a more progressive variation. Fig. 3 shows the amplitude response of a channel that belongs to the first type, registered in the detached house with a link distance of about 40m. In addition to the frequency notches typical in power-line channels (horizontal narrow dark bands), the time variation over the 20ms of mains cycle can be clearly noticed.

This result can be analyzed, to give an insight, in both the frequency and time dimension. Fig. 4a depicts the difference between the channel attenuation at two instants of the cycle corresponding to different response states: 5ms and 10ms. Changes of several dBs are observed at many frequencies. In fig. 4b, the time variation of the frequency response amplitude is plotted at two frequencies: 1.42MHz and 4.59MHz respectively. Now, the evolution during the cycle is more clear, at least for the second frequency that exhibits a two-state behavior with more than 15dBs

between them. At 1.42MHz, it seems that there are no significant variations in the magnitude. However, the phase response has strong changes (of π rad) during the cycle, as seen in fig. 5, where the frequency response is plotted in the complex plane (marks represent the value of the frequency response at each of the *L* intervals). Actually, the phase at this frequency exhibits the two-state behavior as well, with quite fast transitions, as the reduced number of points outside the blurred zones reveals. Phase variations are quite heterogeneous, as can be seen in another curve also drawn in fig. 5, which has been extracted from a channel measured in a different scenario (the apartment). In this case, the shape of the time variation is more gradual, but very remarkable, describing a path during the cycle that covers two quarters of the complex plane. One of the most noteworthy consequences that can be inferred from these results is that channel periodic variations would make difficult to detect signals with QAM constellations unless a time-varying compensation is made.

## 5. RECEIVED NOISE CHARACTERIZATION

The most suitable model to represent electrical appliances noise is a cyclostationary random signal, whose statistical parameters have a slow time variation, synchronous with mains [12].

A random signal $X(t)$ is wide-sense cyclostationary if both its mean and autocorrelation are periodic functions with period $T_0$, in this case the period is 20ms. Moreover, the Fourier transform of the autocorrelation function $R_X(t,t+u)$, called the instantaneous PSD [11], is periodic as well

$$S_X(t,f) = \int_{-\infty}^{+\infty} R_X(t,t+u)e^{-j2\pi fu}du \tag{5}$$

When a cyclostationary random signal $X(t)$ is applied to a slow time-varying system, the instantaneous PSD of the output signal, $Y(t)$, can be approximated by (see section A.2.2),

$$S_Y(t,f) \approx |H(t,f)|^2 \, S_X(t,f) \tag{6}$$

This equation represents a locally linear time-invariant filtering at a time $t$ within mains cycle. It can be used if the autocorrelation function of the input signal and the system impulse response

are both limited to an interval shorter than the channel coherence time.

It should be highlighted that even if a device generates only stationary noise, due to the time-varying filtering of the network, it would become cyclostationary at the receiver.

### 5.1. Measurement methodology

In order to estimate the instantaneous PSD of the noise received from a certain outlet of the power network, a data acquisition card has been plugged to it through the coupling circuit. The captured data, which extend over hundreds of mains cycles, are processed with a spectral estimation algorithm based on periodogram averaging [15]. Since the signal is not stationary, there is no overlapping between the periodograms and they are averaged in a cyclic way to provide a spectrogram along the mains period $T_0$.

The acquired signal, $y(n)$, is divided into $L$ intervals per cycle $c$ among the total number of registered cycles $C$. Each of these intervals has a duration $T_\ell = T_0/L$, which constitutes the time resolution of the spectrogram. The truncated signal in the $\ell$-th interval of the $c$-th cycle is,

$$y_{c,\ell}(n) = y(2NLc + 2N\ell + n),\ 0 \le n \le 2N-1 \tag{7}$$

and its corresponding periodogram is given by,

$$P_c(\ell,k) = \frac{1}{2N}\frac{1}{U}\left|\sum_{n=0}^{2N-1} w(n)y_{c,\ell}(n)e^{-j\frac{2\pi}{2N}kn}\right|^2 \tag{8}$$

where $w(n)$ is a Hanning window of $2N$ samples and $U$ is the normalization factor that removes estimation bias [15].

An estimate of the time and frequency sampled version of the noise instantaneous PSD has been obtained by performing a synchronized averaging of the periodograms in (8),

$$\hat{S}_N(\ell,k) = \frac{1}{C}\sum_{c=0}^{C-1} P_c(\ell,k) \tag{9}$$

with $1/T_s$=50Msamples/s, $N = 512$, $\Delta f = 1/(2T_sN) \simeq 48.8$kHz, $L = 976$ intervals in a cycle and $T_\ell \simeq 20.5\,\mu$s. However, due to the coupler bandwidth, the estimate in (9) is valid only for the values $22 \le k \le 409$.

### 5.2. Representative results

In this subsection a measurement result from the university building is included as an example. In fig. 6, the noise instantaneous PSD found at a certain outlet is depicted. There are remarkable variations in both time and frequency dimensions. These changes can be better observed in fig. 7, which contains two additional curves that correspond to the expected values taken in each dimension: time and frequency.

On one hand, the function in fig. 7a is an estimate of the time average of $S_N(t,f)$ over $T_0$,

$$< S_N(t,f) >= \frac{1}{T_0} \int_{-T_0/2}^{T_0/2} S_N(t,f)dt \tag{10}$$

which is called the PSD of the cyclostationary signal [11]. As seen, noise energy is mainly concentrated in low and medium frequencies, with a notable reduction over 15MHz. On the other hand, in fig. 7b, the expected value of instantaneous PSD over all frequencies gives an estimate of noise power evolution over mains cycle. There is an important excursion, exceeding 15dBs, with a periodicity of 100Hz and a well-defined shape, probably due to the superposition of the noise caused by different devices.

## 6. STATISTICAL ANALYSIS OF CHANNEL TIME VARIATION

Previous subsections have displayed examples of cyclic changes found in the channels registered during the measurement campaign. However, although all the measured channels show a time-varying behavior, not all of them present such significant changes along the cycle. In order to evaluate the real importance of the channel cyclic variations, a statistical analysis of the results obtained in this trial is now presented. Specifically, channel frequency response and noise instantaneous PSD are examined.

### 6.1. Frequency response

In the study of the frequency response time variation, two parameters have been employed: the first one reflects the peak excursion of the changes, while the second one quantifies their rate.

The peak excursion is a parameter commonly employed in the characterization of real signals.

This concept can be extended to a complex signal like the frequency response of the channel by defining,

$$H_{pp}(f) = \max_{t_1,t_2} \left\{ \left| H(t_1, f) - H(t_2, f) \right| \right\} \tag{11}$$

with $t_1, t_2 \in [0, T_0)$. This parameter has a straightforward geometrical interpretation that can be observed in fig. 5, where the values of $H(t,f)$ for a fixed $f = f_i$ and $0 \le t < T_0$ were represented. In this plot, $H_{pp}(f_i)$ corresponds to the distance between the two points that are further away in the complex plane. However, to allow the comparison among peak excursions of different frequencies and channels, it is better to express $H_{pp}(f)$ relative to the time-averaged value of the frequency response amplitude, leading to

$$\widetilde{H}_{pp}(f) = \frac{H_{pp}(f)}{< \left| H(t,f) \right| >} \tag{12}$$

The values of $\widetilde{H}_{pp}(f)$ have been computed for all the frequencies of the whole set of measured channels [2]. Afterwards, they have been grouped in subsets according to the scenario (apartment, detached house and university building) where their corresponding frequency response was measured. Fig. 8 depicts an estimate of the cumulative distribution function (cdf) associated to each subset and to the overall set of frequencies and channels. For clarity, the values of $\widetilde{H}_{pp}(f)$ have been expressed as a percentage. In all the scenarios, the frequency response presents peak excursions greater than 10% in approximately 40% of the cases. However, it should be noted that due to the high frequency selectivity of time variations, the presented cdfs are biased by those frequencies in which the response is nearly invariant [13], i.e. significant peak excursions measured in certain bands (e.g. see Fig. 4.b ) are masked.

The second parameter in this study tries to quantify the rate of channel time variation. It has been estimated by measuring the spectral broadening at the channel output when it is excited with a sinusoid. In mobile radio channels this figure is usually referred to as Doppler spread. In an LPTV channel, the spectral broadening manifests as discrete components harmonically related to

2- It is common to encounter notches in channels amplitude response at certain frequencies. These points have been removed when processing the data because their values are neither significative nor reliable.

$1/T_0$ around the input frequency. In this case, a sort of Doppler spread, $B_D(f)$, can be defined as the largest non-zero Fourier series coefficient of the frequency response,

$$H^{\alpha}(f) = \frac{1}{T_0} \int_{-T_0/2}^{T_0/2} H(t,f) \cdot e^{-j\frac{2\pi}{T_0}\cdot\alpha\cdot t} dt \tag{13}$$

Since $H(t,f)$ is estimated from real measurements, $H^{\alpha}(f)$ [3] is non-zero for all values of $\alpha$. Hence, $B_D(f)$ has been taken as the frequency of the largest coefficient for which $H^{\alpha}(f)$ has reduced 40dB below its maximum, $H^{0}(f)$ [16].

Again, the values of $B_D(f)$ have been computed for all the frequencies of the whole set of measured channels and grouped in subsets according to the scenario in which they were measured. Fig. 9 shows the estimated cdf associated to each scenario, where the quantized nature of $B_D(f)$ at multiples of $1/T_0$ is reflected in the staircase shape of the curves. It is worth noting that not only in 50% of the frequencies the Doppler spread can be even greater than 100 Hz, but also in 10% of the frequencies (except for the apartment channels) $B_D(f)$ values are above 400Hz.

Provided that the interval over which the channel can be considered approximately invariant is inversely related to the Doppler spread, the values in fig. 9 reveal that this interval is no smaller than $600\mu s$ ($\approx 1/1700$). Therefore, these results assure the validity of the measurement procedure used to estimate the channel frequency response, based on the assumption that channel coherence time was longer than the time resolution $T_\ell$=20.5μs.

As previously suggested, cyclic variations in the channel response are generally frequency selective, i.e., $\widetilde{H}_{pp}(f)$ and $B_D(f)$ are clearly "colored" functions for a given channel. This can be highlighted by calculating the rms Doppler spread of each measured channel,

$$B_D rms = \left[ \overline{\left( B_D(f) - \overline{B_D(f)} \right)^2} \right]^{1/2} \tag{14}$$

---

3 - Where $\alpha$ does not represent exponentiation when applied to a function or variable.

where $\overline{(\cdot)}$ stands for the ensemble average over all frequencies of the considered channel. Fig. 10 shows the estimated cdf of the values of $B_D rms$ corresponding to each channel of the three scenarios. For clarity, the values in (14) have been expressed normalized by the average Doppler spread of the channel, $\overline{B_D(f)}$. As seen, no channel experience less than 40% of relative variation, and 50% of them suffer changes up to 140%.

Results presented in this subsection may be of considerable interest for the design of any digital communication system. In particular, for a DMT system, which is considered by now the most appropriate technique for such frequency-shaped channels [3], they have a straightforward implication. Values of $\widetilde{H}_{pp}(f)$ and $B_D(f)$ can be helpful parameters to determine the dynamic range and rate of adaptation needed for the taps of the frequency equalizer (FEQ) commonly employed in DMT. Moreover, the Doppler spread provides very useful information to determine the maximum number of carriers that still guarantees the coherence of the channel during the symbol period.

### 6.2. Noise instantaneous PSD

Following a similar procedure to the one employed with the frequency response, the cyclostationary behavior of the noise instantaneous PSD has been characterized by means of two parameters. The first one reflects the peak excursion of the noise instantaneous PSD and is defined by

$$S_{N\,pp}(f) = \max_t \left\{10\log_{10}\left[S_N(t,f)\right]\right\} - \min_t \left\{10\log_{10}\left[S_N(t,f)\right]\right\} \quad (dB) \tag{15}$$

with $t \in [0, T_0)$. The second one quantifies the rate of change of the noise instantaneous PSD and is computed according to

$$\Delta S_N(f) = \max_t \left\{\left|10\log_{10}\left[S_N(t+T_\ell,f)\right] - 10\log_{10}\left[S_N(t,f)\right]\right|\right\} \quad (dB) \tag{16}$$

with $t \in [0, T_0)$. The estimated cdf of the values given by (15) and (16) have been plotted in fig. 11 and fig. 12, respectively. As seen, approximately in 20% of the situations noise peak excursion exceeds 10dB, of which up to 3dB may occur in just 20.5μs. Furthermore, it is also

worth noting that the laboratory and the apartment are the environments with the highest values of both parameters for most percentiles. In the laboratory this can be due to the high number of devices connected to the grid. In the apartment, channels are established over shorter and less branched links than in the detached house, due to its smaller size. Therefore, cyclostationary noise components reach most outlets with a level that clearly exceeds the one of the background stationary noise.

## 7. CONCLUSIONS

In this paper, cyclic short-time variation of indoor PLC channels has been discussed. It has been justified that the origin of this phenomenon resides in the behavior of some devices, which depends on mains voltage. In particular, measurements performed over tens of common electrical devices support a general description of the loads connected to the grid in terms of a time-varying impedance and a cyclostationary noise source. It has been demonstrated, both empirically and analytically, that these conditions lead to a channel model composed of an LPTV system and an additive cyclostationary noise term. Moreover, it has been shown that a slow-variation approach can be used to simplify the channel analysis.

Based on this framework, a measurement procedure capable of extracting the cyclic time variations, has been described. Representative examples extracted from measurements performed in different scenarios have been shown. In addition, a statistical analysis of the results obtained from this trial has been included. Statistics that reflect the peak excursion and the rate of change of the frequency response and noise instantaneous PSD have been discussed. Presented parameters have validity for any actual power-line channel, since time variation is due to the electrical devices behavior. Therefore, they should be taken into consideration to design broadband digital communication systems. Specifically, in case that a DMT transmission system is used, they can be remarkably helpful to design synchronization procedures, to develop an adaptive frequency equalizer (FEQ), to determine the maximum number of carriers that still

guarantees the channel coherence during the symbol period and to design adaptive transmission schemes that take advantage of the channel periodicity.

## A. APPENDIX: Analytical framework of PLC channels cyclic behavior.

The analysis of PLC channels, which in principle should be seen as nonlinear systems, admits a twofold simplification: the first one is to model them as LPTV systems and the second one is to calculate their response from a sequence of states in which the system behaves as LTI.

### A.1. PLC channels as LPTV systems

Provided that PLC channels contain some nonlinear elements, the most accurate model to describe their behavior is a nonlinear system (NLS). Such systems can be characterized by a Volterra series, expressed as,

$$\begin{aligned} y(t) = h_0 + \int_{-\infty}^{+\infty} h_1(\tau)x(t-\tau)d\tau + \int_{-\infty}^{+\infty} h_2(\tau_1,\tau_2)x(t-\tau_1)x(t-\tau_2)d\tau_1 d\tau_2 + \ldots \\ + \int_{-\infty}^{+\infty}\ldots\int_{-\infty}^{+\infty} h_k(\tau_1,\tau_2,\ldots\tau_k)[\prod_{i=1}^{k} x(t-\tau_i)d\tau_i] + \ldots \end{aligned} \tag{17}$$

where $x(t)$ and $y(t)$ are respectively the system input and output signals, and the terms $h_k(\tau_1,\tau_2,...,\tau_k)$ are called the Volterra kernels. In PLC channels the input is composed of two components $x(t) = s(t) + c(t)$, the small signal $s(t)$ and the large one $c(t)$, and hence, the output signal is,

$$\begin{aligned} y(t) = h_0 + \int_{-\infty}^{+\infty} h_1(\tau)[c(t-\tau) + s(t-\tau)]d\tau \\ + \int_{-\infty}^{+\infty}\int_{-\infty}^{+\infty} h_2(\tau_1,\tau_2)[c(t-\tau_1) + s(t-\tau_1)][c(t-\tau_2) + s(t-\tau_2)]d\tau_1 d\tau_2 + \ldots \end{aligned} \tag{18}$$

In practice, PLC transmission systems include a high-pass filter to protect the receiver from mains voltage, shown in fig. 13, which removes all terms in $y(t)$ that do not contain $s(t)$, that is,

$$z(t) = \int_{-\infty}^{+\infty} h_1(\tau)s(t-\tau)d\tau + \int_{-\infty}^{+\infty} h_2(\tau_1,\tau_2)s(t-\tau_1)s(t-\tau_2)d\tau_1 d\tau_2 + 2\int_{-\infty}^{+\infty} h_2(\tau_1,\tau_2)s(t-\tau_1)c(t-\tau_2)d\tau_1 d\tau_2 \ldots \tag{19}$$

Since kernels magnitude decreases as their order *n* increases and the level of signal $s(t)$ is very low, it is reasonable to neglect also the terms in which $s(t)$ appears more than once,

$$z(t) \simeq \int_{-\infty}^{+\infty} h_1(\tau)s(t-\tau)d\tau + 2\int_{-\infty}^{+\infty} s(t-\tau_1)\int_{-\infty}^{+\infty} h_2(\tau_1,\tau_2)c(t-\tau_2)d\tau_2 d\tau_1 ... \\ = \int_{-\infty}^{+\infty} h_1(\tau)s(t-\tau)d\tau + 2\int_{-\infty}^{+\infty} s(t-\tau_1)f_1(t,\tau_1)d\tau_1 ... \quad (20)$$

where,

$$f_1(t,\tau_1) = \int_{-\infty}^{+\infty} h_2(\tau_1,\tau_2)c(t-\tau_2)d\tau_2 \;;... \quad f_2(t,\tau_1) = \int_{-\infty}^{+\infty}\int_{-\infty}^{+\infty} h_3(\tau_1,\tau_2,\tau_3)c(t-\tau_2)c(t-\tau_3)d\tau_2 d\tau_3 \;;... \quad (21)$$

The first term in (20) corresponds to an LTI behavior, but the others represent an LTV behavior, since the output depends on the instant when the input is applied. Equation (20) can be reformulated in the following way,

$$z(t) \simeq \int_{-\infty}^{+\infty} h_1(\tau)s(t-\tau)d\tau + 2\int_{-\infty}^{+\infty} f_1(t,t-\tau)s(t-\tau)d\tau + 3\int_{-\infty}^{+\infty} f_2(t,t-\tau)s(t-\tau)d\tau + ... \\ = \int_{-\infty}^{+\infty} [h_1(\tau) + 2f_1(t,t-\tau) + 3f_2(t,t-\tau) + ...]s(t-\tau)\,d\tau \quad (22)$$

Let us denote $h(t,t-\tau) = h_1(\tau) + 2f_1(t,t-\tau) + 3f_2(t,t-\tau) + ...$, so that (22) can be written in the usual way of an LTV system response [17], as it is also indicated in fig. 13,

$$z(t) \simeq \int_{-\infty}^{+\infty} h(t,t-\tau)s(t-\tau)d\tau \quad (23)$$

Moreover, the time-varying character of the system response $h(t,t-\tau)$ is only due to the mains signal $c(t)$, as seen in (21), which is periodic in time and so the system is LPTV.

**A.2. Slow-variation approximation for PLC channels**

The LPTV behavior of PLC channels exhibits peculiar characteristics that facilitate the analysis. The time variation is usually quite slow and has a very long period, $T_0$=20ms. The following slow-variation approach holds whenever channel coherence time is longer than both channel delay spread (what is usually called an "underspread" channel) and duration of input signal [12].

***A.2.1. Slow-variation LPTV filtering: deterministic signals***

Since channel response $h(t,t-\tau)$ is periodic in time, it can be expanded in Fourier series,

$$h(t,t-\tau) = \sum_{\alpha=-\infty}^{+\infty} h^{\alpha}(\tau)e^{j2\pi\alpha t/T_0} \quad (24)$$

When the system is excited by an input signal $x(t)$, the response is given by

$$y(t) = \int_{\infty}^{+\infty} h(t,t-\tau)x(t-\tau)d\tau = \sum_{\alpha=-\infty}^{+\infty}\int_{\infty}^{+\infty} h^{\alpha}(\tau)x(t-\tau)d\tau \cdot e^{j2\pi\alpha t/T_0} = \sum_{\alpha=-\infty}^{+\infty} y^{\alpha}(t)e^{j2\pi\alpha t/T_0} \quad (25)$$

In the last equation two factors can be observed: the first one, $y^{\alpha}(t)$, of fast variation (at transmission information rate fixed by $x(t)$), and the second one, the complex exponential, much slower (according to the mains cycle). Under this circumstances, the latter factor can be assumed approximately constant during a certain time interval denoted as $t \approx \sigma$ (i.e. $t \in [\sigma - \Delta t, \sigma + \Delta t]$ with $\Delta t$ small). This approximation is also grounded in that response coefficients $y^{\alpha}(t)$ tend to zero as α tends to infinite. Thus, when a short-time signal (in relation to the channel coherence time) situated in $t \approx \sigma$, $x_{\sigma}(t)$, is applied, the system output will change depending on the instant within mains cycle at which input is applied, that is,

$$y(t) \simeq y_{\sigma}(t) \simeq \sum_{\alpha=-\infty}^{+\infty} y_{\sigma}^{\alpha}(t) e^{j2\pi\alpha\sigma/T_0} \tag{26}$$

At this point, Fourier transformation can be used to translate (26) to frequency domain,

$$Y_{\sigma}(f) \simeq \sum_{\alpha=-\infty}^{+\infty} Y_{\sigma}^{\alpha}(f) e^{j2\pi\alpha\sigma/T_0} = \sum_{\alpha=-\infty}^{+\infty} H^{\alpha}(f) X_{\sigma}(f) e^{j2\pi\alpha\sigma/T_0} = X_{\sigma}(f) \sum_{\alpha=-\infty}^{+\infty} H^{\alpha}(f) e^{j2\pi\alpha\sigma/T_0} \tag{27}$$

where coefficients $Y^{\alpha}(f)$ are related to the Fourier transform of the input signal $X_{\sigma}(f)$ by, (see (25)),

$$Y_{\sigma}^{\alpha}(f) = H^{\alpha}(f) \cdot X_{\sigma}(f) \tag{28}$$

Finally, by taking into account the Fourier series of the LPTV system frequency response,

$$H(t, f) = \sum_{\alpha=-\infty}^{+\infty} H^{\alpha}(f) e^{j2\pi\alpha t/T_0} \tag{29}$$

the frequency domain relation of the slow-variation LPTV filtering process is obtained,

$$Y_{\sigma}(f) \simeq H(t, f)|_{t=\sigma} \cdot X_{\sigma}(f) \tag{30}$$

The input signal can be always made as short as desired, simply putting a long-time signal as the combination of several shorter ones and recombining the outputs to these. Hence, the necessary condition for (29) to hold is that the system remains invariant during the effective length of its impulse response.

### *A.2.2. Slow-variation LPTV filtering: random signals*

A cyclostationary signal $X(t)$ has a periodic instantaneous PSD, $S_X(t, f)$, defined in (5), which can be expanded in Fourier series of coefficients $S_X^{\alpha}(f)$. In PLC channels, cyclostationary noise

has a period equal to the one of the LPTV channel, $T_0$, what simplifies the analysis.

When an LPTV system is excited by a cyclostationary signal of its same period, the output is also cyclostationary and its instantaneous PSD has the following coefficients [11,12],

$$S_Y^{\alpha}(f) = \sum_{\beta=-\infty}^{+\infty} \sum_{\gamma=-\infty}^{+\infty} \left[ H^{\beta}\left( f - \frac{\alpha+\beta}{T_0} \right) \right]^* H^{\gamma}\left( f - \frac{\gamma}{T_0} \right) S_X^{\alpha+\beta-\gamma}\left( f - \frac{\gamma}{T_0} \right) \tag{31}$$

In practice, due to the system slow-variation, the factors in (30) can be approximated as,

$$H^{\beta}\left( f - \frac{\alpha+\beta}{T_0} \right) \simeq H^{\beta}(f); \quad H^{\gamma}\left( f - \frac{\gamma}{T_0} \right) \simeq H^{\gamma}(f); \quad S_X^{\alpha+\beta-\gamma}\left( f - \frac{\gamma}{T_0} \right) \simeq S_X^{\alpha+\beta-\gamma}(f) \tag{32}$$

This expression holds true unless integers values $\alpha, \beta$ and γ take extremely high values. Even if this happens, it is compensated by the fact that $H^{\beta}(f)$ strongly decreases as $\beta$ increases, so only low order coefficients are significant. The first two approximations in (32) state that the channel frequency selectivity is smaller than a frequency shift corresponding to the significant harmonics of $1/T_0$ (the frequency-domain counterpart of the slow-variation condition), while the latter one implies that the autocorrelation of $X(t)$ must be of short duration compared to the channel coherence time.

As a consequence of (32), (31) can be simplified,

$$S_Y^{\alpha}(f) = \sum_{\beta=-\infty}^{+\infty} [H^{\beta}(f)]^* \cdot \sum_{\gamma=-\infty}^{+\infty} H^{\gamma}(f) S_X^{\alpha+\beta-\gamma}(f) \tag{33}$$

where the second factor is a convolution sum in the coefficients domain that has been represented by $\odot$ to reformulate (33),

$$S_Y^{\alpha}(f) \simeq \sum_{\beta=-\infty}^{+\infty} [H^{\beta}(f)]^* \cdot \left[ H^{\alpha+\beta}(f) \odot S_X^{\alpha+\beta}(f) \right] = [H^{-\alpha}(f)]^* \odot H^{\alpha}(f) \odot S_X^{\alpha}(f) \tag{34}$$

Finally, by using the synthesis equation of the Fourier series for the input and output instantaneous PSD and channel frequency response (29), this relation turns into,

$$S_Y(t,f) \simeq H^*(t,f) \cdot H(t,f) \cdot S_X(t,f) = |H(t,f)|^2 \, S_X(t,f) \tag{35}$$

**ACKNOLEDGMENT**

This work has been partially supported by the Spanish Ministry of Educación y Ciencia under Project TIC2003-06842.

## 8. REFERENCES


[1] H. Philipps, "Performance measurements of power-line channels at high frequencies," in *International Symposium on Power-Line Communications and its Applications* (ISPLC), 1998, pp. 229–237.

[2] K. Dostert, *Powerline Communications.* Prentice Hall, 2001.

[3] F.J. Cañete, J.A. Cortés, L. Díez, and J.T. Entrambasaguas, "Modeling and evaluation of the indoor power line channel," *IEEE Communication Magazine*, vol.41, pp. 41–47, April 2003.

[4] D. Liu, E. Flint, B. Gaucher and Y. Kwark, "Wide band AC power line characterization," *IEEE Trans. Consumer Electronics*, Vol. 45, pp. 1087–1097, November 1999.

[5] H. Philipps, "Modelling of power line communication channels," in *International Symposium on Power-Line Communications and its Applications* (ISPLC), 1999, pp. 14–21.

[6] M. Zimmermann and K. Dostert, "A Multipath Model for the Powerline Channel," *IEEE Trans. on Communications,* 553-559, pp., April 2002.

[7] I.C. Papaleonidopoulos, C.N. Capsalis, C.G. Karagiannopoulos, N.J. Theodorou, "Statistical analysis and simulation of indoor single-phase low voltage power-line communication channels on the basis of multipath propagation," *IEEE Transactions on Consumer Electronics*, Vol. 49, pp. 89 – 99, February 2003.

[8] G. Marubayashi, S. Tachikawa, "Spread spectrum transmission on residential power line," in *IEEE 4th International Symposium on Spread Spectrum Techniques and Applications*, 1996, Vol.3, pp. 1082-1086.

[9] M. Zimmermann and K. Dostert, *"*Analysis and modeling of impulsive noise in broad-band powerline communications*," IEEE Trans. on Electromagnetic Compatibility*, pp. 249–258, February 2002.

[10] F.J. Cañete, J.A. Cortés, L. Díez, J.T. Entrambasaguas and J.L. Carmona, "Fundamentals of the cyclic short-time variation of indoor power-line channels" in *International Symposium on Power-Line Communications and its Applications* (ISPLC), 2005, pp. 157-161.

[11] W.A. Gardner, *Introduction to Random Processes*. MacMillan, 1986.

[12] F.J. Cañete, *Caracterización y modelado de redes eléctricas interiores como medio de transmisión de banda ancha*, Ph.D. Thesis, University of Málaga, 2004. ISBN: 84-689-1003-1.

[13] J.A. Cortés, F.J. Cañete, L. Díez and J.T. Entrambasaguas, "Characterization of the cyclic short-time variation of indoor power-line channels response" in *International Symposium on Power-Line Communications and its Applications* (ISPLC), 2005, pp. 326-330.

[14] O. Edfors, M. Sandell, J.J. Van de Beek, D. Landström and F. Sjöberg, "An introduction to orthogonal-frequency division multiplexing," *Research Report 1996:16,* Division of Signal Processing, Luleå University of Technology, September 1996.

[15] A. Oppenheim and R. Schafer, *Discrete-Time Signal Processing*. Prentice Hall, 1989.

[16] S.J. Howard and K. Palavan, "Doppler spread measurements of indoor radio channel", *Electronics Letter*, Vol. 26, No. 2, January 1990, pp. 107-108.

[17] R.E. Crochiere and L.R. Rabiner. *Multirate Digital Signal Processing.* Prentice Hall, 1983.

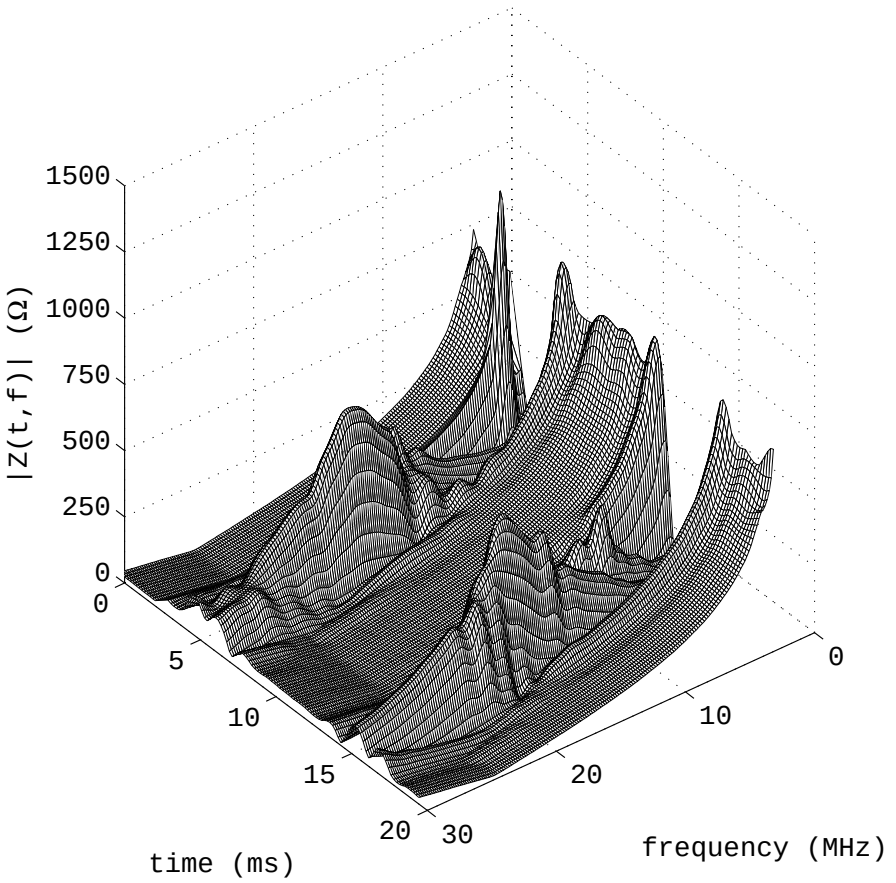


**Fig. 1. Time variant impedance of an electrical device.**

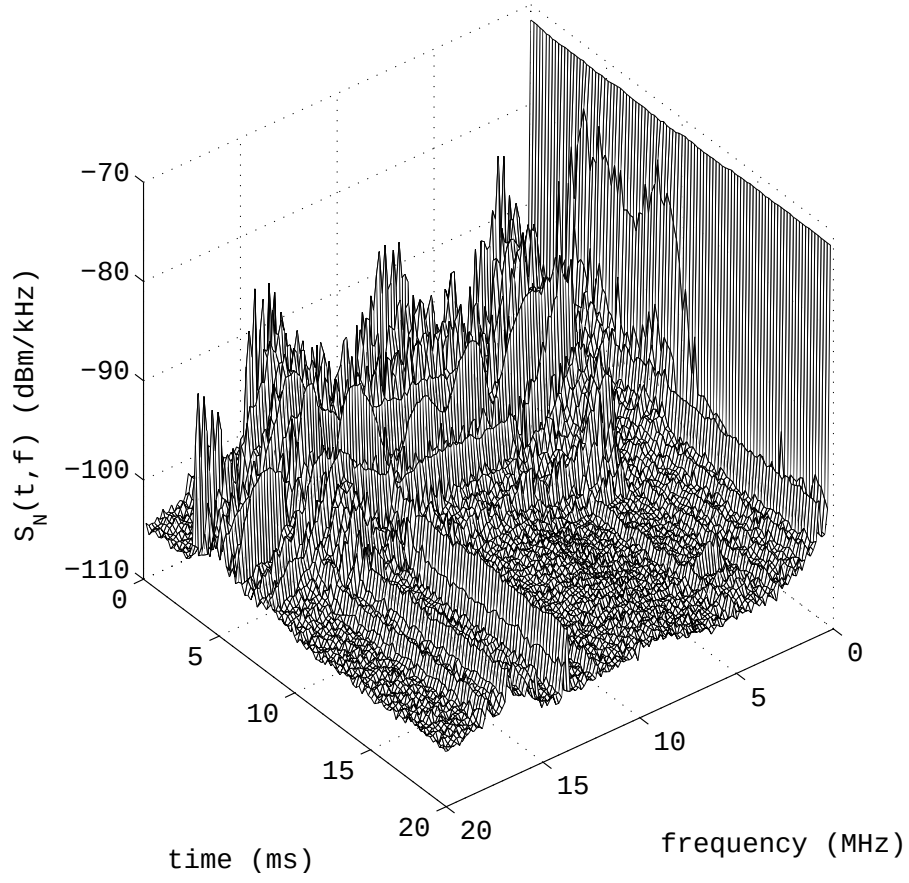


**Fig. 2. Cyclostationary noise instantaneous PSD generated by an electrical appliance**

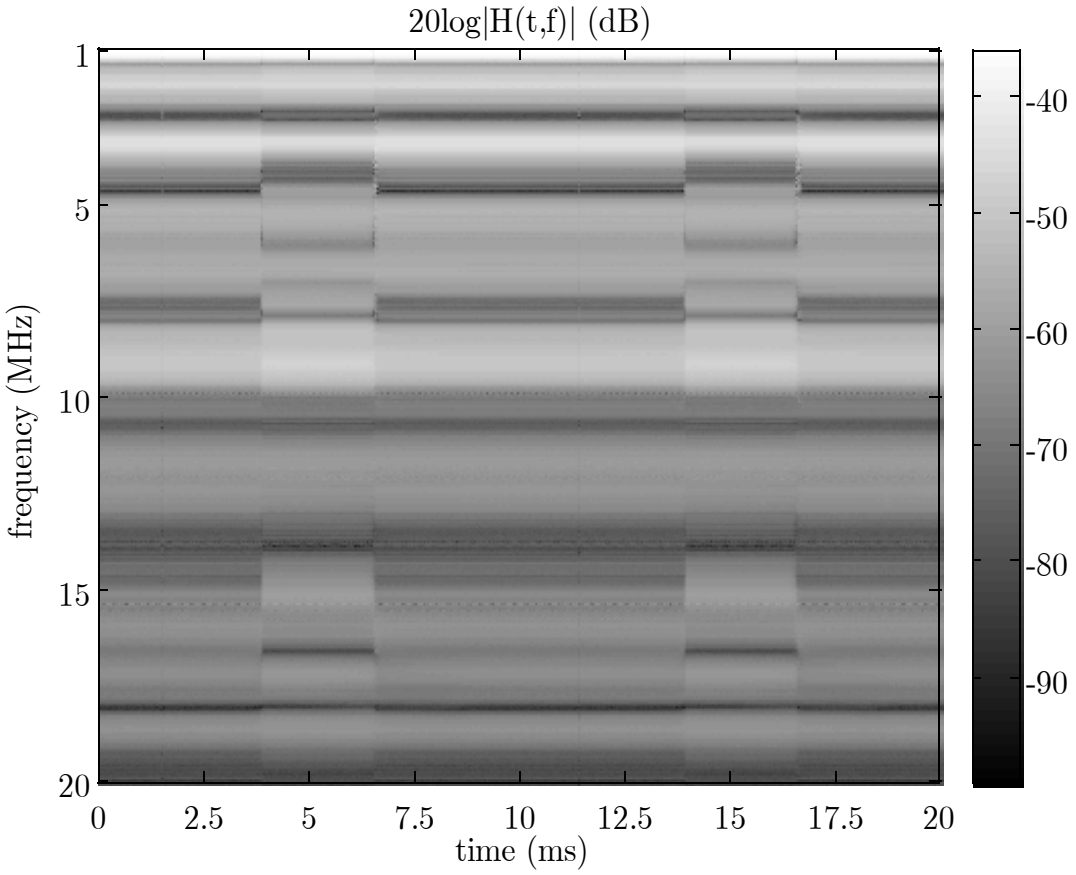


**Fig. 3. Cyclic amplitude response of a channel measured in a detached house**

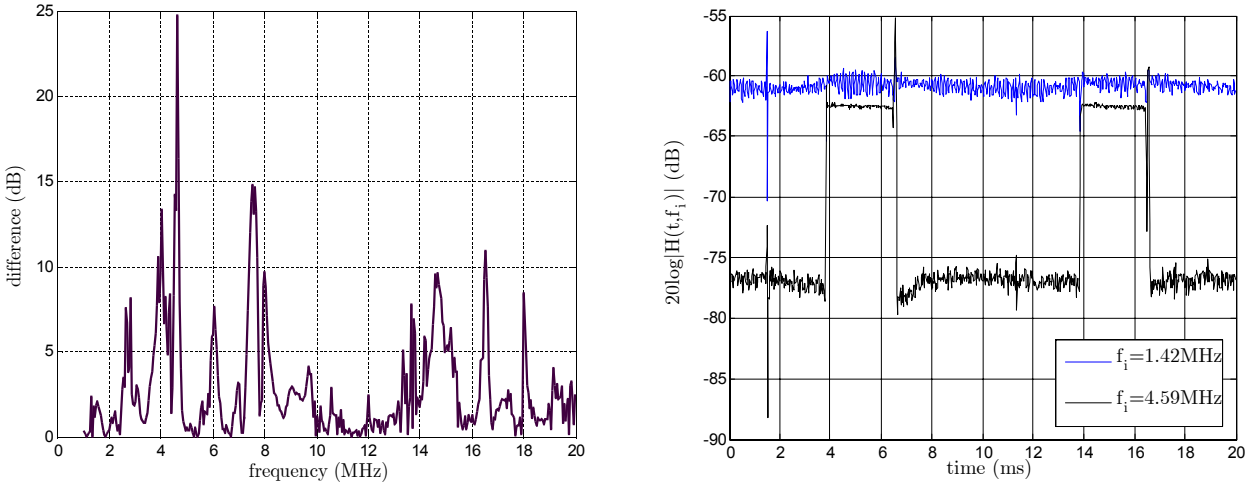


**a)** **b)**

**Fig. 4. Analysis of frequency response in fig. 3, a) difference of the amplitude for two instants of the mains cycle: at 5ms and 10ms; b) magnitude evolution along the mains cycle for two frequencies**

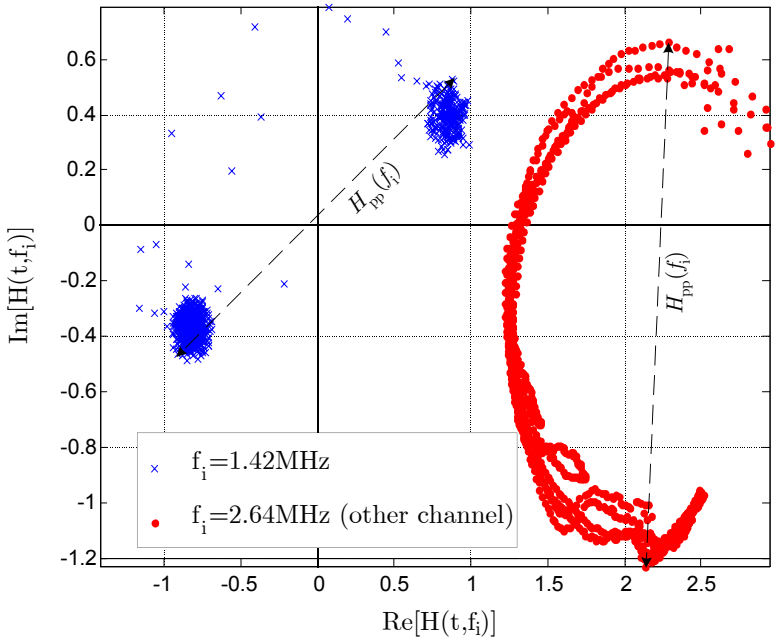


**Fig. 5. Normalized complex value of the frequency response in fig. 3 at f=1.42MHz along the mains cycle; and the same representation for the frequency response of another channel in an apartment at f=2.64MHz.**

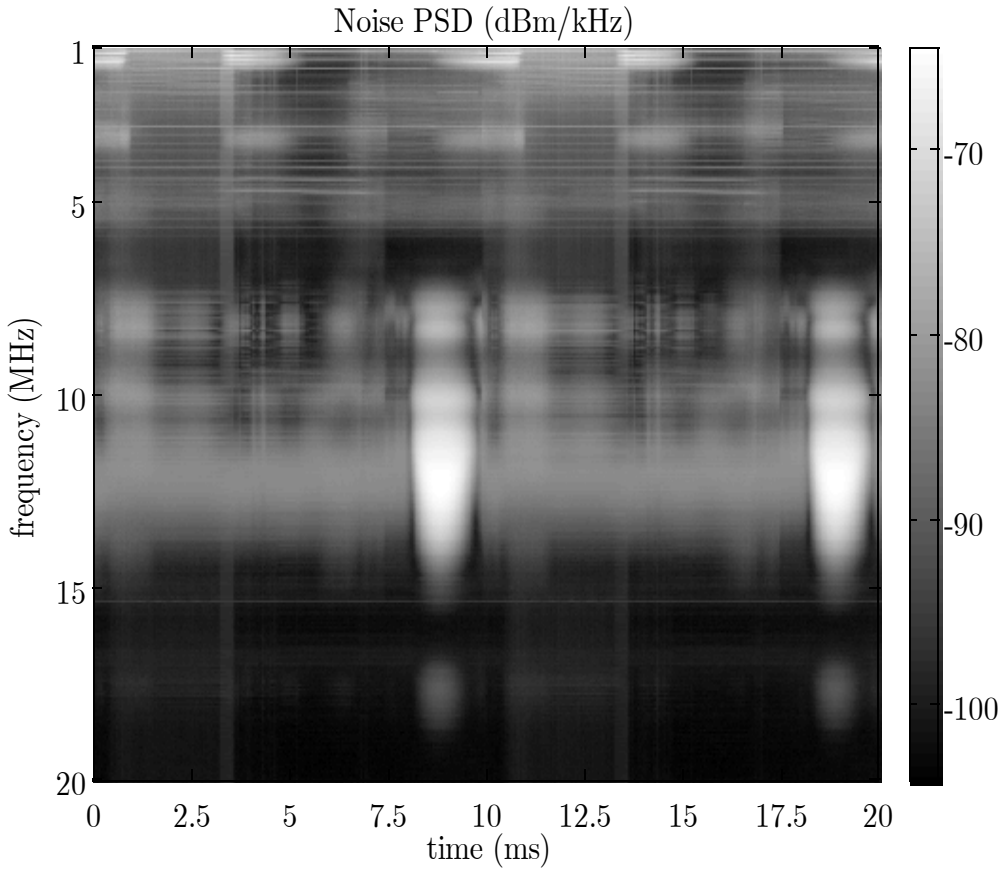


**Fig. 6. Noise instantaneous PSD measured in a university channel**

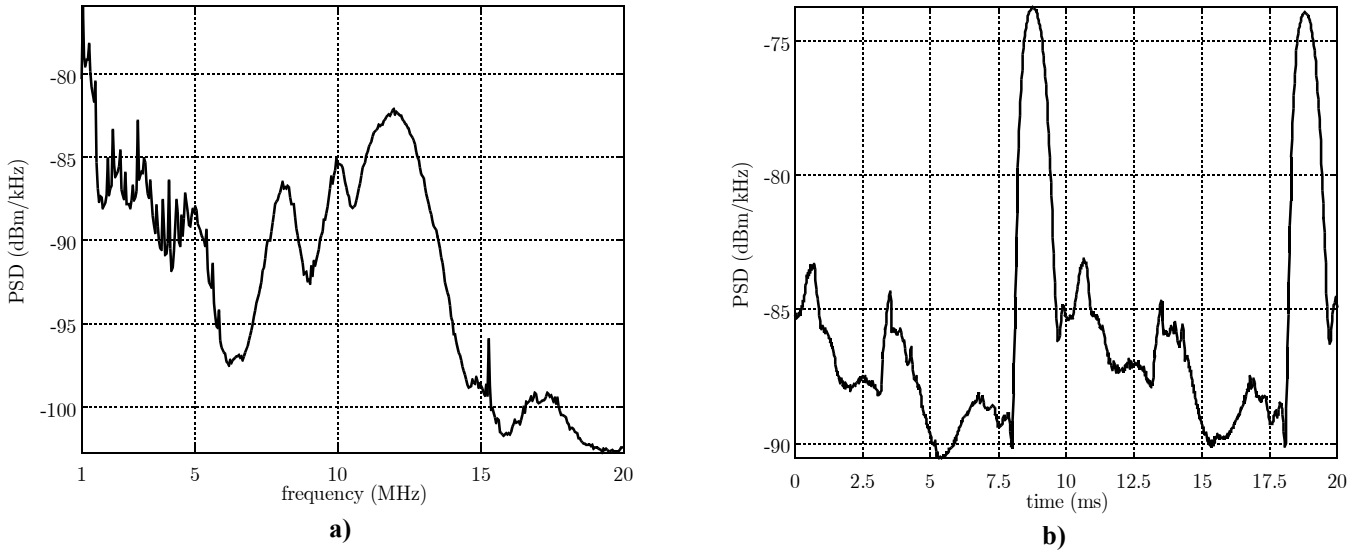


**Fig. 7. Expected value of PSD in Fig. 6: a) applied to time dimension b) applied to frequency dimension**

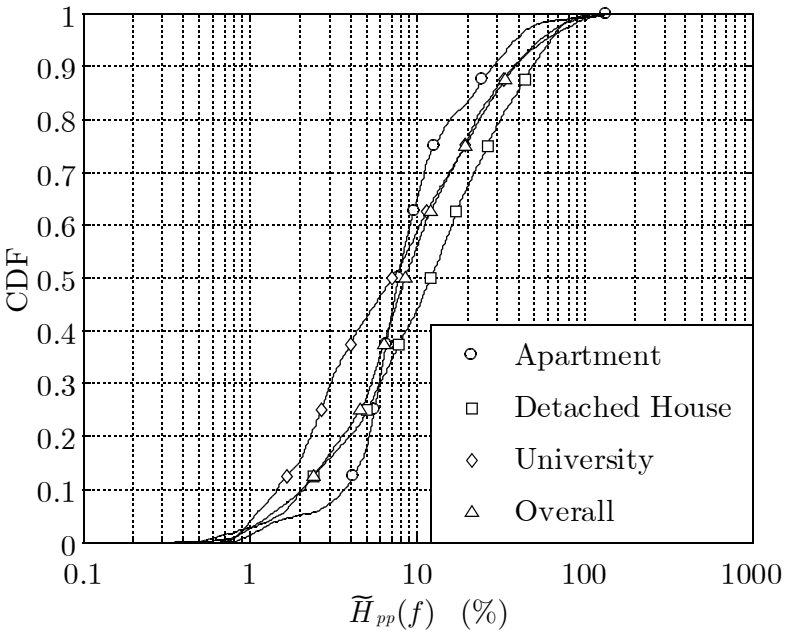


**Fig. 8. Cdf of the relative peak excursion of the frequency response expressed as a percentage**

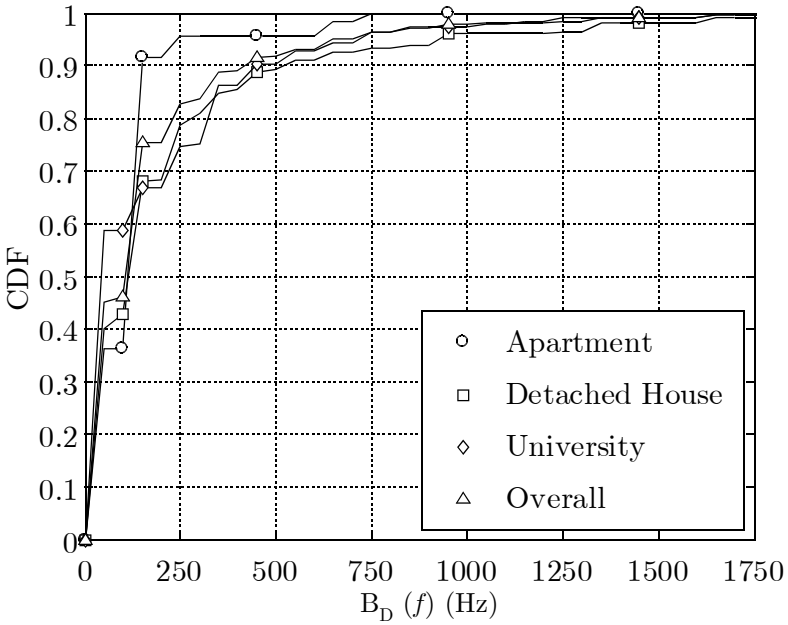


**Fig. 9. Cdf of the Doppler spread**

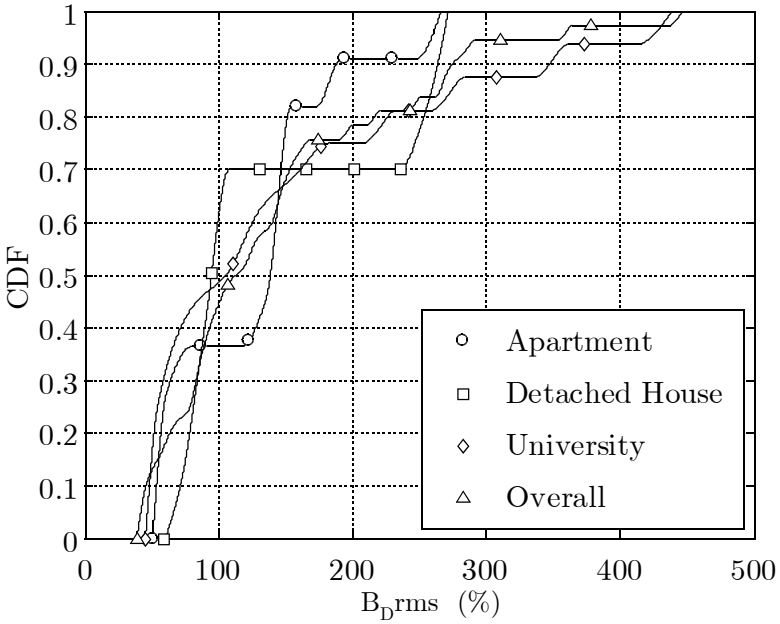


**Fig. 10. Cdf of the rms Doppler spread of each measured channel**

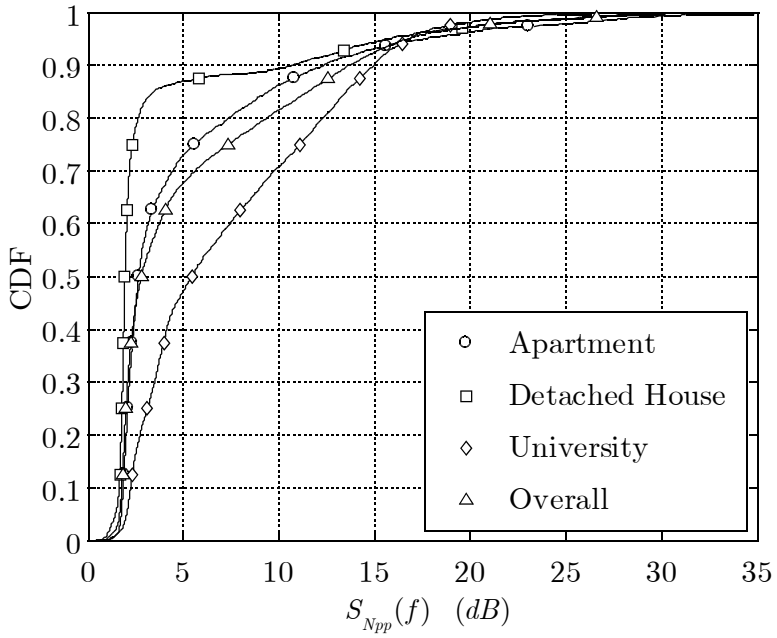


**Fig. 11. Cdf of the peak excursion of the noise instantaneous PSD**

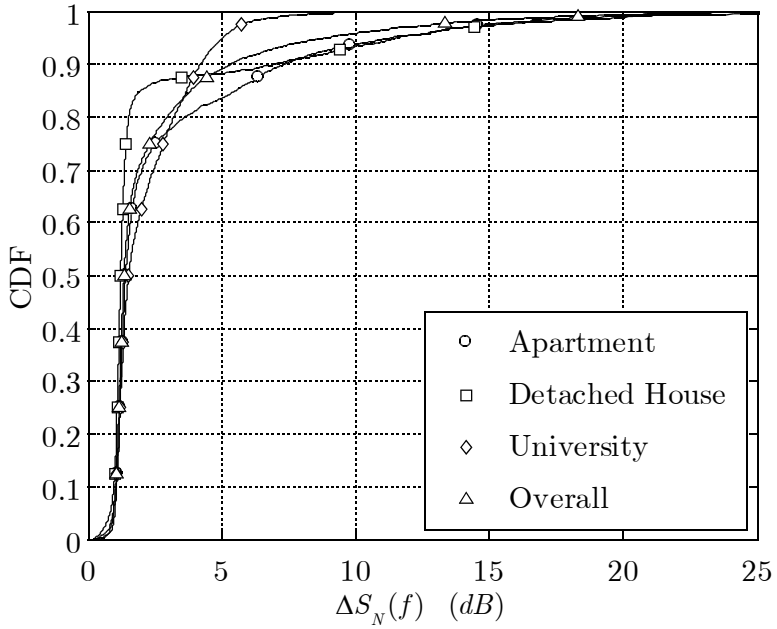


**Fig. 12. Cdf of the rate of change of the noise instantaneous PSD**

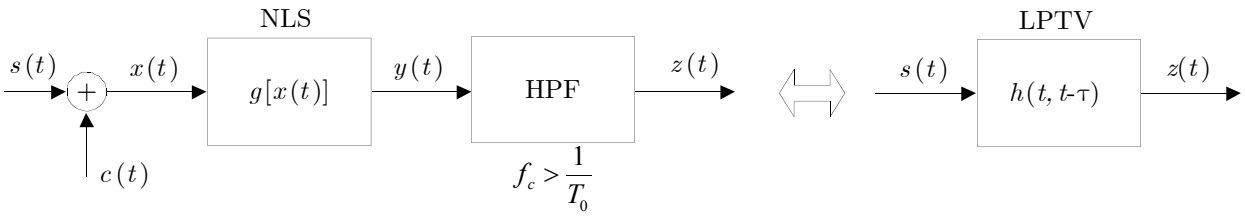


**Fig. 13. Diagram of the LPTV approximation of PLC channels seen as nonlinear systems**